

## **MODERN ELECTROCHEMICAL PROCESSES AND TECHNOLOGIES IN IONIC MELTS**

**A. Omelchuk, S. V. Volkov and O. G. Zarubitskii**

Institute of General and Inorganic Chemistry, Ukrainian National Academy of Sciences,  
32-34 Palladina avenue, 03680 Kiev 142, Ukraine

*(Received 18 January 2003; accepted 2 March 2003)*

### **Abstract**

*An analysis of the known methods for the electrochemical purification of non-ferrous metals in ionic melts is presented. A comparative estimation of the results of the electrochemical purification of non-ferrous metals by different methods has been performed. The main regularities of the electrochemical behavior of non-ferrous metals in conventional and electrode micro-spacing electrolysis are presented. It has been found that when electrolyzing some metals, e. g. bismuth, gallium, there is either no mass exchange between the electrodes, or it occurs under filtration conditions. It has been shown that the electrode micro-spacing processes provide a high quality of non-ferrous metals purification at low specific consumption of electric power and reagents. The use of bipolar electrodes and  $\beta$ -alumina diaphragms hinders the transfer of metallic impurities from the anode to the cathode. The effects revealed were used to develop new processes for the separation of non-ferrous metal alloys in ionic melts; most of them have been put into practice in non-ferrous metallurgy.*

*Keywords:* ionic melts, electrochemical processes, non-ferrous metals, purification

### **1. Introduction**

The present development level of science and technology calls for creating new technologies, particularly, in the fields of power supply and new materials production. The demand for new materials doubles approximately every 11 years. At such growth rates

of consumption, mineral deposits are rapidly depleted. According to experts' estimations, as early as at the beginning of this millennium, the deposits of the most important mineral raw materials will be practically fully depleted. They include deposits of almost all non-ferrous and noble metals. The deposits of energy carriers: petroleum, natural gas, uranium-235 will have a somewhat longer exploitation time. The time of exploitation of nickel, molybdenum, and manganese deposits is estimated to be about 100 years. The iron deposits can be exploited three times longer; the chromium reserves must last about 500-600 years. The coal reserves are now the largest ones (over 800 years). Under these circumstances, the creating of new technologies for producing metals and compounds based on them, as well as new materials from secondary raw materials is a topic of not only practical but also scientific interest.

The research carried out in recent years shows that considerable progress in this direction can be achieved by using ionic melts as reaction media [1-25, 29, 30]. Electrochemical processes in ionic melts ensure:

- a high mass exchange rate through effecting chemical and electrochemical transformations in the liquid phase (the operating temperature range is 210 to 1000 °C) and the possibility to use high current densities (up to  $1 \times 10^4 \text{ Am}^{-2}$ ) and compounds in lower oxidation states;
- high metal extraction selectivity and purification quality through the possibility to effect metal transfer both from anode to cathode and in the opposite direction (Table 1), to use bipolar electrodes [19-21,23] and special materials, for example, modified  $\beta$ -alumina [23,24, 34];
- low specific consumption of electric energy and reagents through the possibility to effect mass exchange between the electrodes at very small electrode spacings (of the order of 0.5-1.0 mm) [5-9].

Analysis of the capabilities of known electrochemical technologies [1,3,4-29] has shown electrode micro-spacing electrochemical processes in molten electrolytes, or so-called thin-layer electrolysis [7,9], to be most suitable for the solution of the above problems. In contrast to the conventional electrolysis, it makes it possible to effect 1, 3, and 4 variants (see Table 1) of mass exchange between the electrodes. The conventional one permits to realize only the first and second variants (Table 1).

## 2. Results and discussion

The essence of electrode micro-spacing electrochemical processes in molten electrolytes is that mass exchange between the electrodes is effected across thin (about 0.5-1.0 mm thick) porous materials, which prevent, owing to surface tension forces, mixing of the molten metal phases. The electrode spacing is equal to the thickness of the porous material, and the amount of the electrolyte being in its pores is quite sufficient for stable mass exchange between the electrodes. To separate the molten metal phases from the

Table 1. Variants of mass exchange in ionic melt electrolysis

Variants	Transfer	Processes at the electrodes		References
		at the cathode	at the anode	
1	Conventional transfer (from anode to cathode)	$Me_1^{n+} + ne^- = Me_1^0$	$Me_1^0 = Me_1^{m+} + ne^-$	[26, 27]
2	Intermetallide transfer (from cathode to anode)	$Me_2^{l+} + le^- = Me_2^0$ $xMe_2 + yMe_1 = Me_{2x}Me_{1y}$	$Me_{2x}Me_{1y} =$ $= xMe_2 + yMe_1^{n+} + yne^-$	[26-28]
3	Without mass exchange	$Me^{m+} + (m-n)e^- = Me^{n+}$	$Me^{n+} = Me^{m+} + (m-n)e^-$	[1, 11, 12]
4	Under filtration conditions	Change in surface tension	Change in surface tension	[1, 13]

electrodes, heat-resistant silica, basalt, carbon materials (cloths, ceramics) and  $\beta$ -alumina are used. Such materials can bear a layer of molten metal, which exerts a pressure of over 6000 N/m<sup>2</sup>, without leakage, making it possible to create commercial electrochemical reactors. A schematic diagram of thin-layer electrochemical reactor is shown in Fig.1. Performed investigations show that the current density at the electrodes in reactors of this type can go beyond  $1 \times 10^4$  Am<sup>-2</sup> without short circuit. Also, the current efficiency for the overwhelming majority of low-melting non-ferrous metals corresponds (within the determination error) to the theoretical value, obtained from the assumption that equilibrium phases form according to the phase diagram. In contrast to the conventional electrolysis, the surfaces of the molten metal electrodes in micro-spacing electrolysis are parallel to each other, which ensures uniform distribution of current density, mass exchange rate and temperature.

Fig.2 shows schematic diagram of a conventional “crucible-in-crucible” electrolyzer [26-28] and the distribution of current density on the electrode surfaces and the electroactively active constituent over the electrolyte layer thickness [29,30]. From the data given it is evident that the true values of current density in different areas of the electrodes differ greatly from the values calculated for the geometric area. This circumstance does not allow processes of metals purification and alloys separation to be purposively controlled.

The possibility to effect electrolysis at very small electrode spacing allows the specific consumption of electric energy and electrolyte to be substantially reduced. For example, in indium refining the specific consumption of electric energy decreases by a factor of 1.6-2.0 and that of the electrolyte by a factor of 175-200 [6,8].

The features of mass transfer across porous materials make it also possible to considerably decrease impurity transfer from anode to cathode and to improve thereby the quality of metal purification. Characteristics of indium purification by the ordinary and micro-spacing electrolysis are listed in Table 2.

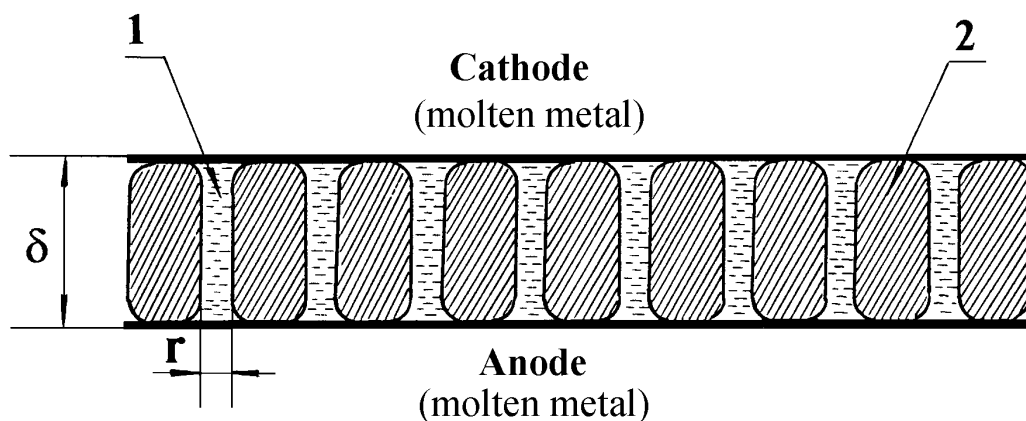


Figure 1. Schematic diagram of electrode micro-spacing electrochemical process: (1) electrolyte (ionic melt); (2) fibers (matrix) of heat-resistant materials;  $r$ , pore diameter;  $\delta$ , porous material thickness;  $\delta > r = (0.5-1.0) \times 10^{-3}$  m.

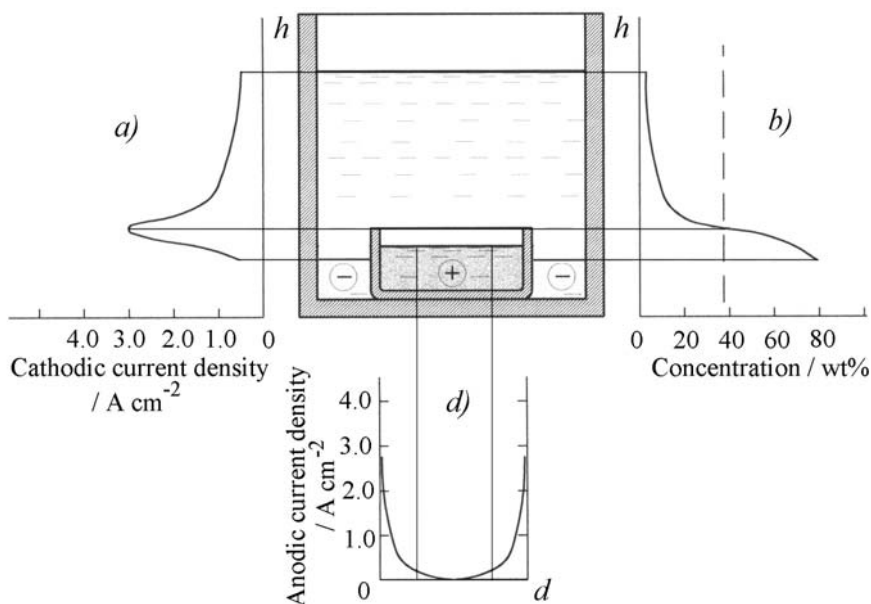


Figure 2. Schematic diagram of a "crucible-in-crucible" electrolyzer and current density distribution at the cathode (a), at the anode (d) and electromotively active constituent concentration distribution (b) over the electrolyte layer thickness ( $h$ ) and anodic chamber width ( $d$ ) in the case of separation of a lead-bismuth alloy ( $I=1800$  A,  $t=480$  °C).

Table 2. Comparative characterization of indium purification by the conventional and electrode micro-spacing electrolysis ( $i=1600 \text{ Am}^{-2}$ ,  $t=220 \text{ }^\circ\text{C}$ )

Metallic impurity	Impurity content (wt %)		
	Before purification	After purification	
		Conventional electrolysis	Electrode micro-spacing electrolysis
Pb	0.03	0.003	0.0004
Sn	0.02	0.001	0.0002
Cu	0.02	0.0001	0.00001
Ni	0.01	0.0001	0.00002

The observed effect may be accounted for by the difference in the mechanism of mass transfer between the electrodes in the former and latter cases. Mass transfer in an electrolyte is known [31] to take place through diffusion ( $j_D$ ), migration ( $j_M$ ), and convection ( $j_C$ ). Accordingly, the total flow  $j_\Sigma$  is:

$$j_\Sigma = j_D + j_M + j_C \quad (1)$$

Taking into account the fact that in the case of micro-spacing electrolysis the whole interelectrode space is filled with a porous material and the electrodes are in a close proximity to each other, the contribution of convection may be neglected in the first approximation, whereas in the case of conventional electrolysis this cannot be done. The contribution of convection to mass exchange may be schematically illustrated as follows (Fig.3). The electrolyte layer between the electrodes may be conventionally divided into three zones:  $0\delta_1$  and  $\delta_2L$ , near- electrode zones with stationary electrolyte (diffusion layers);  $\delta_1\delta_2$ , zone with convective agitation. According to the Nernst convective diffusion theory, concentration change takes place mainly within the confines of diffusion layers. In the case of stationary electrolysis, it can be approximated, under certain conditions, by the first Fick's law. In the zone with convective agitation, the concentration of a substance is generally considered to be constant throughout the whole volume. In the case of conventional electrolysis, the variation of metallic impurity concentration between the electrodes is represented by broken line 1, and its value at the cathode is  $10C_{3i}^C$ . In the idealized case, in an entirely stationary electrolyte, this dependence is approximated by the straight line 2. The impurity concentration at the cathode in this case is  $12C_{3i}^C$ , which is much lower than the concentration  $13C_{3i}^C$ . The real dependence of impurity concentration on the electrode spacing is represented by curve 3. Accordingly, the impurity concentration at the cathode,  $14C_{3i}^C$ , will be somewhat higher than in the idealized case but much lower than in the conventional electrolysis.

The metallic impurity concentration distribution between the electrodes in the case of micro-spacing electrolysis can be assessed by solving the set of differential equations:

$$\frac{\partial C_i}{\partial t} = -\text{div } j_{\Sigma} = -\text{div}(j_D + j_i) \quad (2)$$

$$i = -n_i F j_{\Sigma} \quad (3)$$

with the condition that the electroneutrality of the electrolyte:

$$\sum_i C_i z_i = 0 \quad (4)$$

is retained.

The exact solution of this set of equations for real multi-component electrolytes is

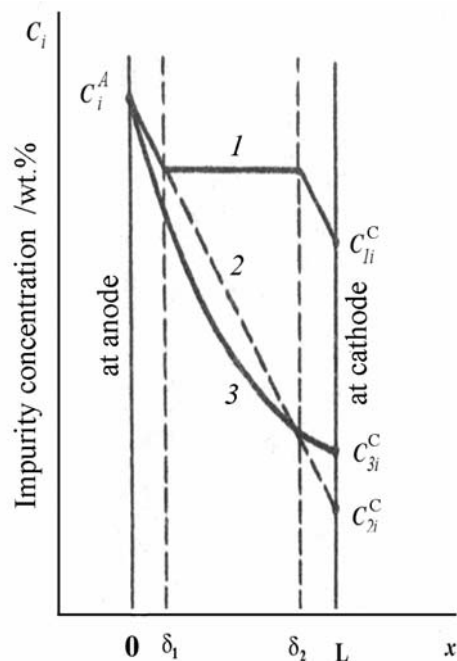


Figure 3. Metallic impurity concentration distribution between the electrodes in the case of electrolysis with convective transfer (1), in the idealized case without it (2), and in the case of electrode micro-spacing electrolysis (3).

rather complicated, therefore appropriate restrictions were imposed [7], which are satisfied under appropriate electrolysis conditions. The electrolysis is conducted under galvanostatic conditions with non-polarizable electrodes of the same metal. The anode

contains tenths of a percent of metallic impurity. The ion flow of the metal being refined,  $j_l$ , is much larger than that of metallic impurity,  $j_i$ . During the electrolysis, the concentration of the metal being refined in the electrolyte layer is not changing. For these conditions, the following metallic impurity concentration distribution between the electrodes has been obtained:

$$\frac{C_i^C}{C_i^A} = \frac{\exp\left(\frac{z_i F}{RT} \cdot \frac{l}{\beta} \cdot \frac{ir}{\chi_0}\right)}{1 - A_i \left[1 - \exp\left(\frac{z_i F}{RT} \cdot \frac{l}{\beta} \cdot \frac{ir}{\chi_0}\right)\right]} \quad (5)$$

where  $C_i^C$  and  $C_i^A$  are the impurity concentration at the cathode and anode respectively,  $l$  is pore length,  $\beta$  is pore tortuosity coefficient,  $r$  is the resistance coefficient of the material that fills the interelectrode space,  $\chi_0$  is electrolytic conductivity,  $A_i$  is a constant that characterizes exchange reactions at interfaces. For metallic impurities with more positive electrode potential than that of the metal to be refined,  $A_i > 1$ , and with more negative electrode potential,  $A_i < 1$ .

Eq.(5) makes it possible to predict the results of electrolysis depending on its conditions. Increasing the parameters  $i$ ,  $l$ , and  $r$  must decrease the impurity transfer from the anode to the cathode. In this case, the ratio  $C_i^C/C_i^A$  approaches the limit  $1/A_i$ .

Analysis of experimental data, which have been obtained both under laboratory conditions and on commercial reactors, confirms the reliability of the prediction results [6-8]. Fig.4 shows the dependence of the ratio  $C_i^C/C_i^A$  on current density at the electrodes in indium refining, which was determined experimentally (curves 1, 2, 3) and calculated from Eq.(5) (curve 4). From the data given it is obvious that in both cases this ratio decreases symmetrically with increasing current density.

Table 3 lists the results of zinc purification by electrode micro-spacing electrolysis. From the data given it is evident that impurity transfer from the anode to the cathode decreases with increasing current density and thickness of the porous dielectric, as it was expected according to predictions on the basis of Eq.(5). The diaphragm material does not practically affect the purification quality. Better results were achieved in a binary electrolyte (mixture of zinc and potassium chlorides), where the difference in electrode potential between zinc and metallic impurities is larger as compared with ternary electrolyte (mixture of zinc, potassium and sodium chlorides) [16-20]. Specific electric energy consumption in an electrolyte with higher electric conductivity (binary electrolyte) is 1.4-1.6 kWh per kg of zinc and in that with lower conductivity 1.8-2.0 kWh per kg of zinc, whereas in conventional electrolysis this characteristic reaches 3.0 kWhkg<sup>-1</sup>.

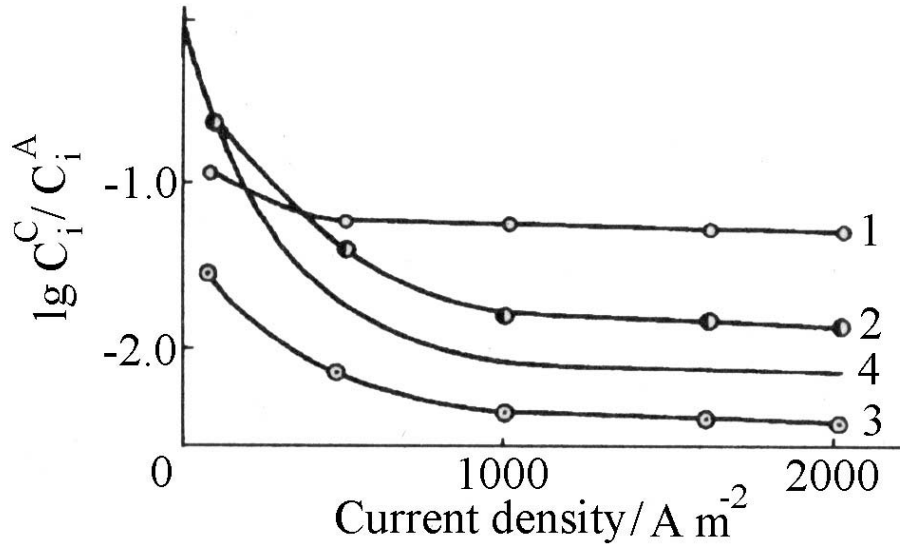


Figure 4. Dependence of the ratio  $C_i^C/C_i^A$  on current density in the case of removing the impurities Sn (1), Pb (2), and Cu (3) from indium at 220 °C; (4) result of calculation by equation (5) at  $A=100$ .

Table 3. Results of zinc purification by electrode micro-spacing electrolysis (impurity level of crude zinc, wt. %: Bi- $2 \times 10^{-2}$ , Pb- $6 \times 10^{-2}$ , Cu- $1 \times 10^{-2}$ , Fe -  $5 \times 10^{-2}$ )

Electrolysis conditions					Impurity level of purified zinc (wt. % $\times 10^3$ )				
Current density $\times 10^3$ (Am $^{-2}$ )	$t$ (°C)	Electrolyte composition	Diaphragm material	Diaphragm thickness $\delta \times 10^{-4}$ (m)	Pb	Cu	Sn	Fe	Bi
0.5	500	Ternary	Silica	0.5	1.0	1.0	2.0	1.0	3.0
0.5	500	---	Basalt	1.0	4.0	5.0	8.0	4.0	8.0
1.0	500	---	Silica	0.5	0.5	0.7	0.3	0.6	0.4
5.0	500	---	---	0.5	0.6	0.5	0.2	0.5	0.3
1.0	480	Binary	---	1.0	0.3	0.2	0.1	0.2	0.1
2.0	550	---	---	1.0	0.3	0.1	0.2	0.2	0.1



The electrode micro-spacing electrolysis makes it possible to use a liquid bipolar electrode (Fig.5) [20, 21, 23]. The essence of such an electrolysis is that under the action of direct current, the metal being purified dissolves at the anode, transfers through the electrolyte layer to the cathode surface and the bipolar electrode, where it is reduced to metal. Then, it diffuses to the anode surface, and dissolves again in the electrolyte layer. After the transport through the second electrolyte layer, the metal being purified is reduced again at the cathode. Metallic impurities accumulate in the anode residue and bipolar electrode. The number of discharge-ionization operations depends on the number of bipolar electrodes. Bipolar electrode electrolysis enables deposition of metals with an impurity content of  $(1-8) \times 10^{-5} \%$  [19-21,23,24].

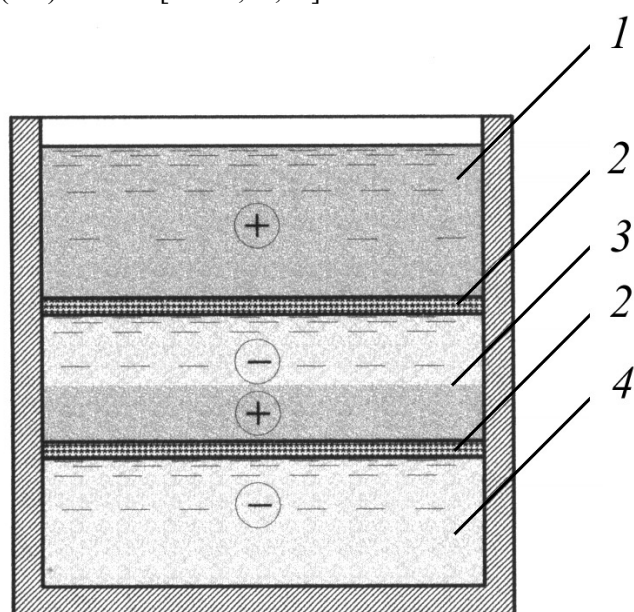


Figure 5. Schematic diagram of an electrochemical reactor with bipolar electrode: (1) anodic metal, (2) porous dielectric, (3) bipolar electrode, (4) cathodic metal.

Analyzing electrode micro-spacing electrochemical processes, one should point out features of the electrochemical behavior of such metals as bismuth and gallium.

Among the heavy non-ferrous metals, bismuth has one of the most positive electrode potentials, therefore it remains on the anode in electrolysis, and impurities are extracted into the electrolyte layer and onto the cathode. It is known [26,27] that during electrolysis in chloride melts, bismuth is contaminated with chloride due to the interaction:



The amount of this impurity may reach 5-6 % depending on electrolysis conditions and time. The loss of the metal in this case is 10-15 %. Electrode micro-spacing electrochemical processes substantially reduce these characteristics thanks to the very small volume of the electrolyte layer [10,11].

Comparative characterization of bismuth purification by thin-layer and ordinary electrolysis is given in Table 4.

*Table 4. Comparative characterization of electrochemical purification of bismuth by conventional and electrode micro-spacing electrolysis in ionic melts*

Process parameters	Purification method	
	Conventional method	Electrode micro-spacing electrolysis
Specific electrical energy consumption, kW h/kg	0.09-0.12	0.03-0.04
Specific electrolyte consumption, kg/kg	1.5-2.0	0.03-0.05
Loss of bismuth, %	10-15	<1.5
Optimum current density, Am <sup>-2</sup>	1000	2000
Chlorine impurity content, %	5.0-6.0	0.7-0.8

When investigating the electrochemical behavior of bismuth and impurities in the electrode micro-spacing electrochemical processes, it was found [8,11,12] that under certain conditions, there is no mass exchange between the electrodes after extracting the metals with more negative potentials. Owing to interaction (6), compounds of bismuth in different oxidation states are formed in the electrolyte layer. Since electrolysis takes place in a confined and closed space, and the electrodes are closely spaced concentration gradient of these compounds appears between them. Owing to this, compounds of bismuth in lower oxidation states can move to the anode and oxidize at it, and compounds of bismuth in higher oxidation states can move in the opposite direction and be reduced at the cathode. Redox processes are known to involve no metal transfer from anode to cathode.

An evidence of the fact that the absence of metal transfer from anode to cathode does not result from short circuit of the electrodes is the current-voltage characteristic for electrode micro-spacing electrochemical cell, which is non-linear in character (Fig.6). Besides, it has a limiting current region, which is absent from voltammetric curves for conventional cells [12]. In electrode micro-spacing electrochemical processes, in contrast to ordinary electrolysis, conditions are apparently possible when the flows of ions in different oxidation states to the electrodes are equal, which causes the limiting current region to appear.

The effect revealed was used to develop new processes for the separation of non-ferrous alloys [32-34]. The essence of these processes is that the alloys to be separated

are dissolved in bismuth, from which the desired component is then extracted selectively under anodic polarization. In this case, bismuth does not participate in transfer from anode to cathode, and its compounds in different oxidation states control the part of current that is expended on the transfer of the metal with more negative electrode potential.

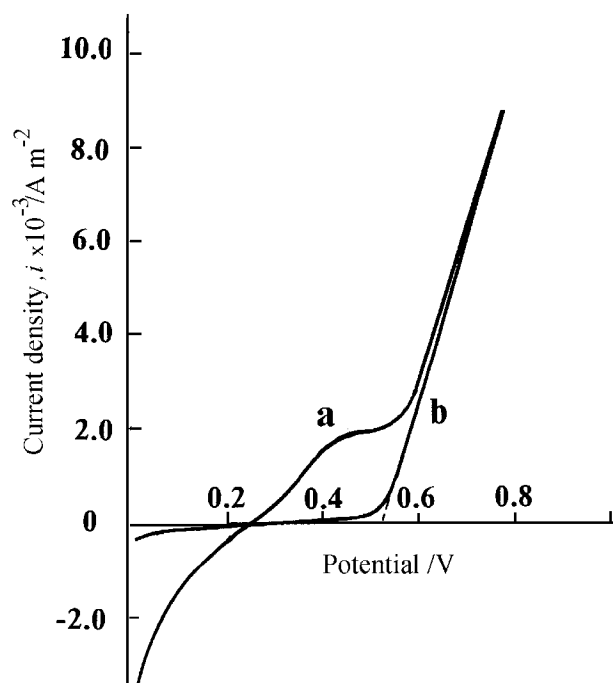
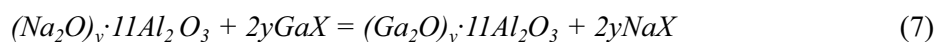


Figure 6. Voltammetric curves for an electrode micro-spacing (a) and conventional (b) electrochemical cell with lead cathode and bismuth anode.

For example, the separation of lead-silver alloys with low silver content (up to 2-5 %) by conventional electrolysis is not very efficient because a considerable amount of silver transfers into the electrolyte and to the cathode. Alloying with bismuth makes it possible to increase the difference in ionization potential between lead and silver. Electrolysis is carried out in two stages [32,34]. In the first stage, lead is extracted from the ternary alloy, silver being concentrated by transfer from the larger volume of lead alloy into the smaller volume of bismuth alloy. The residual concentration of lead in the anodic alloy is  $(3-5) \times 10^{-2}$  wt. % and that of silver in cathodic lead is about  $3 \times 10^{-3}$  wt. %. The end of the process is determined potentiometrically. In the second stage, silver, whose residual concentration in bismuth is 0.2-0.3 %, is extracted. Bismuth that remained on the anode is used in the next operation of the technological process.

Another example of using bismuth as a separator may be the process for the separation of indium antimonide. The intermetallic compound is decomposed by alloying with bismuth at 600-700 °C. This is facilitated to a certain degree by the ability of bismuth to form compounds with indium that are less stable than antimonide [33]. The decomposition results in the formation of a homogeneous ternary alloy, from which indium as a metal with the most electronegative potential is extracted by electrode micro-spacing electrolysis. The direct extraction of indium onto the cathode is 98 %. After extracting antimony from bismuth, the latter is used in the subsequent antimonide decomposition operations.

It was pointed out above that  $\beta$ -alumina can be used to fill the interelectrode space. This material is notable not only for having a high ionic conductivity but also for the possibility of inverse isomorphous substitution of sodium cations by other cations, for example by mono-valent gallium cations, without considerable distortion of the main fragments of the structure of this material [24,35-37]:



where  $X$  stands for halide ions.  $\beta$ -Alumina modified by cations of the metals to be refined decreases the transfer of metallic impurities from anode to cathode. The use of it in gallium refining makes it possible to obtain the metal of 99.9999 % purity with current efficiency close to the theoretical value [23,24,36].

It was pointed out above that the principle of electrode micro-spacing electrolysis makes it possible to effect a variant of mass exchange between the electrodes, the results of which do not obey Faraday laws (Table 1, variant 4). It may be called conditionally transfer “contrary to Faraday”, for the change in mass of the electrodes does not correspond to the quantity of electricity passed through the cell. The principle of electrode micro-spacing electrolysis is effected owing to the fact that surface tension forces do not allow the molten metal to infiltrate through porous dielectric materials that separate the electrodes. When investigating the electrochemical behavior of non-ferrous metals in electrode micro-spacing electrochemical cells, it was found [13] that some metals (e.g. gallium) acquire, under certain polarization conditions, the ability to change the surface tension and, depending on its magnitude, either to leak freely through the porous dielectric material or not. In the case of gallium, this effect manifests itself in hydroxide electrolytes at certain electrode potential values. Anodic polarization of a gallium electrode leads to a decrease in surface tension and to infiltration of gallium through the porous dielectric. Electrode polarization in the opposite direction increases the surface tension, and there is no infiltration.

The effect revealed was used [38] to develop a process for gallium purification by filtration method. It is known [39] that the gallium purification technology involves the operation of filtering off mechanical impurities, which is generally carried out by a

vacuum technique. The use of the electrochemical method makes it possible to avoid the vacuum technique and to greatly simplify this operation.

The advantages of electrode micro-spacing electrochemical processes over the known electrolysis methods proved to be so considerable that they were brought to a commercial level in a very short time [6,40].

## Conclusions

A significant progress in the purification of non-ferrous metals (*Sn, In, Bi, Zn, Ga*, etc.) and separation of their alloys can be achieved by using the electrochemical electrode micro-spacing processes in ionic melts.

The essence of these processes in molten electrolytes is that mass exchange between the electrodes is effected across thin (about 0.5-1.0 mm thick) porous materials, which prevent, owing to surface tension forces, mixing of the molten metal phases. The amount of the electrolyte that is in its pores is quite sufficient for stable mass exchange between the electrodes. To separate the molten metal phases of the electrodes, heat-resistant silica, basalt, carbon materials (cloths, ceramics) and  $\beta$ -alumina are used.

The features of mass transfer in the devices for the realization of electrode micro-spacing processes make it possible not only to reduce substantially the specific electric energy and electrolyte consumption, but also to decrease noticeably the impurity transfer from anode to cathode and hence to improve the quality of metal refining.

The advantages of electrode micro-spacing electrochemical processes over the known electrolysis methods proved to be so considerable that they were brought to a commercial level.

## References

1. O.G. Zarubitskii, Ukrainian Journal of Chemistry, 66 (2000) 5 (in Russian).
2. S.V. Volkov and A.A. Omelchuk, Ukr. J. Chem., 66 (2000) 7 (in Russian).
3. A.G. Morachevsky, Russ. J. Appl. Chem., 72 (1999) 3.
4. A.A. Omelchuk, O.G. Zarubitskii, V.N. Gorbach and V.E. D'yakov, J. Appl. Electrochem., 26 (1999) 277.
5. O.G. Zarubitskii, A.A. Omelchuk, V.G. Budnik, V.T. Melyokhin, and V.N. Gorbach, Non-Ferrous Metals, 5 (1990) 41 (in Russian).
6. A.A. Omelchuk, V.T. Melyokhin, L.A. Kazanbaev, M.N. Kozlov, and A.K. Marchenko, Non-Ferrous Metals, 2 (1992) 22 (in Russian).
7. A.A. Omelchuk, Russ. J. Appl. Chem., 66 (1993) 1704.
8. A.A. Omelchuk, V.G. Budnik, O.G. Zarubitskii, V.T. Melyokhin, and V.N. Gorbach, Russ. J. Appl. Chem., 63 (1990) 555.
9. A.A. Omelchuk and O.G. Zarubitskii, Ukr. J. Chem., 60 (1994) 503 (in Russian).

10. O.G. Zarubitskii, V.G. Budnik, and A.A. Omelchuk, *Russ. J. Appl. Chem.*, 67 (1994) 921.
11. A.A. Omelchuk, O.G. Zarubitskii and V.G. Budnik, *Proc. 5<sup>th</sup> International Symposium on Molten Salt Chemistry and Technology*, 24-29 August, Dresden, Germany, 1997, p. 387.
12. A.A. Omelchuk, V.G. Budnik, and O.G. Zarubitskii, *Ukr. J. Chem.*, 61 (1995) 111 (in Russian).
13. O.G. Zarubitskii, A.A. Omelchuk, and V.G. Budnik, *Russ. J. Appl. Chem.*, 69 (1996) 788.
14. V.F. Kozin and A.A. Omelchuk, *Ukr. J. Chem.*, 63 (1997) 122 (in Russian).
15. V.F. Kozin and A.A. Omelchuk, *Russ. J. Appl. Chem.*, 71 (1998) 1026.
16. V.F. Kozin and A.A. Omelchuk, *Proc. 5<sup>th</sup> International Symposium on Molten Salt Chemistry and Technology*, 24-29 August, Dresden, Germany, 1997, p. 383.
17. A.A. Omelchuk and V.F. Kozin, *Ukr. J. Chem.*, 64 (1998) 37 (in Russian).
18. A.A. Omelchuk and V.F. Kozin, *Russ. J. Appl. Chem.*, 71 (1998) 1903.
19. V.F. Kozin and A.A. Omelchuk, *Environmental Ecology and Resources Saving*, 4 (1999) 21 (in Russian).
20. V.F. Kozin and A.A. Omelchuk, *Reports of Higher Education School, Non-Ferrous Metallurgy*, 1 (1999) 38 (in Russian).
21. V.F. Kozin and A.A. Omelchuk, *Inorganic Materials*, 38 (2002) 270 (in Russian).
22. A.A. Omelchuk and O.G. Zarubitskii, *Electrochimica Acta*, 44 (1999) 1779.
23. V.F. Kozin and A.A. Omelchuk, *Reports of Higher Education School, Non-Ferrous Metallurgy*, 5 (2000) 27 (in Russian).
24. V.F. Kozin and A.A. Omelchuk, *Ukr. J. Chem.*, 66 (2000) 52 (in Russian).
25. V.F. Kozin and A.A. Omelchuk, *Environmental Ecology and Resources Saving*, 1 (2001) 26 (in Russian).
26. Y.K. Delimarskii and O.G. Zarubitskii, *Electrorefining of Heavy Metals in Ionic Melts*, *Metallurgiya*, Moscow, 1975 (in Russian).
27. Y.K. Delimarskii, *Theoretical Fundamentals of Ionic Melt Electrolysis*, *Metallurgiya*, Moscow, 1986 (in Russian).
28. O.G. Zarubitskii, *Purification of Metals in Basic Melts*, *Metallurgiya*, Moscow, 1981 (in Russian).
29. A.A. Omelchuk, O.G. Zarubitskii and V.G. Budnik, *Proc. 2<sup>nd</sup> European East-West Workshop on Chemistry and Energy*, Sintra, Portugal, 1995, p. 173.
30. A.A. Omelchuk, O.G. Zarubitskii, and V.G. Budnik, *Russ. J. Appl. Chem.*, 69 (1996) 443.
31. B.B. Damaskin and O.A. Petrii, *An Introduction to Electrochemical Kinetics*, *Vyshshaya Shkola*, Moscow, 1975 (in Russian).
32. V.G. Budnik, A.A. Omelchuk, V.T. Melyokhin, V.N. Gorbach and V.P. Opanasyuk, *Patent USSR No. 14090991*, 1987 (in Russian).

33. O.G. Zarubitskii, V.V. Geikhman, V.G. Budnik, L.A. Kazanbaev, A.A. Omelchuk, M.N. Kozlov, V.T. Melyokhin, V.N. Gorbach, A.Y. Gaas and B.D. Birman, Patent USSR No. 14786635, 1987 (in Russian).
34. O.G. Zarubitskii, V.G. Budnik, A.A. Omelchuk, V.T. Melyokhin, V.P. Opanasyuk and N.F. Zakharchenko, Russ. J. Appl. Chem, 75 (2002) 572.
35. R.H. Radzilowski, Inorg. Chem., 8 (1969) 994.
36. V.F. Kozin and A.A. Omelchuk, Progress in Molten Salt Chemistry 1, R.W. Berg, H.A. Hjuler (Editors), ELSEVIER, Paris, 2000, p. 275.
37. V.F. Kozin and A.A. Omelchuk, Ukrainian Patent No. 45105, 2001 (in Russian).
38. O.G. Zarubitskii, A.A. Omelchuk, V.G. Budnik, V.T. Melyokhin, and V.N. Gorbach, Ukrainian Patent No. 1356, 1994 (in Russian).
39. M.A. Kolenkova and O.E. Krein, Metallurgy of Disseminated and Light Rare Metals, Metalurgiya, Moscow, 1977 (in Russian).
40. L.A. Kazanbaev, V.V. Geikhman, P.A. Kozlov, and A.K. Marchenko, Non-Ferrous Metals, 5 (2000) 46 (in Russian).